PHYSICAL REVIEW A **69**, 040701(R) (2004)

# Differential ionization cross-section calculations for hydrogenic targets with $Z \leqslant 4$ using a propagating exterior complex scaling method

Philip L. Bartlett* and Andris T. Stelbovics†
*Centre for Atomic, Molecular and Surface Physics, Murdoch University, Perth 6150, Australia*
(Received 10 December 2003; published 14 April 2004)

A propagating exterior complex scaling method, with iterative coupling, has been adapted for the electron impact of charged hydrogenic targets. Using this fully *ab initio* method for solving the Schrödinger equation, which has no uncontrolled approximations, we present highly accurate total, single-differential, double-differential, and triple-differential cross-section calculations for the electron-impact ionization of hydrogenic targets with nuclear charge $Z \leqslant 4$ ($H$, $He^+$, $Li^{2+}$, $Be^{3+}$). For a fixed scaled energy, the total and differential cross sections begin to converge with respect to increasing $Z$ when scaled by $Z^4$ and $Z^6$, respectively, and converge more rapidly with increasing incident-electron energy. The angular distributions of the differential cross sections change systematically with increasing nuclear charge for energies above the peak total ionization cross section, but for some lower-energy kinematics the triple-differential cross section for charged targets is significantly different from that of atomic hydrogen.

DOI: 10.1103/PhysRevA.69.040701 PACS number(s): 34.80.Dp

The electron-impact ionization of hydrogenic ions is of fundamental importance to plasma modeling in astrophysics and nuclear fusion. Due to the small cross sections of these ions, absolute experimental measurements are difficult, especially for differential cross sections. Consequently, plasma modeling is heavily dependent on accurate theoretical calculations. For large nuclear charges $Z$, the total ionization and scattering cross sections are predicted to scale inversely to $Z^4$, and the differential cross sections scale inversely to $Z^6$ [1–3]. A question that remains however is what is the behavior of the ionization cross sections for low $Z$, where the scaling law approximation does not rigorously apply, and at what energies and $Z$ does the scaling law become accurate?

To date, many of the published theoretical calculations for total and differential ionization cross sections for low-$Z$ hydrogenic targets have relied upon approximation methods, including the distorted wave Born approximation [4,5] and the "BBK" method [6,7]. These methods generally provide acceptable approximations when electron correlation effects are less dominant, for example, high-energy collisions or when interparticle separations are large. State-of-the-art methods that are known to provide accurate differential cross sections for the ionization of atomic hydrogen over all energies and kinematics, such as exterior complex scaling (ECS) [8], convergent close coupling (CCC) [9], and time-dependent close coupling (TDCC) [10] are computationally intensive and require significant supercomputing resources. We note that their published calculations for the ionization of hydrogenic targets beyond hydrogen is limited. CCC [11] has only been extended to $He^+$ total ionization cross sections (TICS) and TDCC [12,13] has only been applied to $He^+$ and $Li^{2+}$ TICS; ECS has yet to be applied to charged targets, and none of these methods have reported differential ionization cross sections.

So as to provide accurate total and differential ionization cross sections for low-$Z$ hydrogenic targets, we have adapted our time-independent propagating exterior complex scaling (PECS) method for charged hydrogenic targets. We have recently demonstrated [14] that this method, enhanced by use of an iterative coupling scheme, improves the efficiency of our PECS algorithm by one to two orders of magnitude, and provides highly accurate ionization cross sections for atomic hydrogen. As there are no uncontrolled approximations in the method, we expect that the present calculations are of similar accuracy, and the gain in efficiency of our algorithm has allowed us to undertake this wide-ranging set of calculations. We have concentrated on low-$Z$ calculations at low to moderate energies, where approximate theoretical models are expected to be of limited accuracy, and investigate the conformance of the cross sections to the $Z^4$ and $Z^6$ scaling laws.

Using the PECS method with iterative coupling, we have calculated the scattering wave functions for the electron impact of hydrogenic targets with nuclear charge $Z \leqslant 4$. A detailed description of PECS, for two hydrogen model problems, was presented in Ref. [15]. An overview of this method, with iterative coupling, was given for atomic hydrogen in Ref. [14]. To extend the equations given in these papers for the general case of a ground-state hydrogenic target with nuclear charge $Z$ requires only minor modification to the Hamiltonian operator and the initial-state hydrogen wave function. Also, as the incoming incident electron is moving in an electrostatic field, it must be represented by a Coulomb wave of charge $Z-1$ instead of the plane wave used previously for neutral targets. Using a partial-wave expansion of the outgoing scattering wave function [14] the coupled partial-wave equation for the scattering wave function becomes (in atomic units)

$$(E - \hat{H}_{l_1} - \hat{H}_{l_2})\psi^{LS}_{l_1 l_2}(r_1, r_2) - \sum_{l_1' l_2'} \left\langle l_1 l_2 \left\| \frac{1}{r_{12}} \right\| l_1' l_2' \right\rangle_L \times \psi^{LS}_{l_1' l_2'}(r_1, r_2) = \chi^{LS}_{l_1 l_2}(r_1, r_2), \quad (1)$$

where

*Electronic address: bartlett@fizzy.murdoch.edu.au
†Electronic address: stelbovi@fizzy.murdoch.edu.au

 

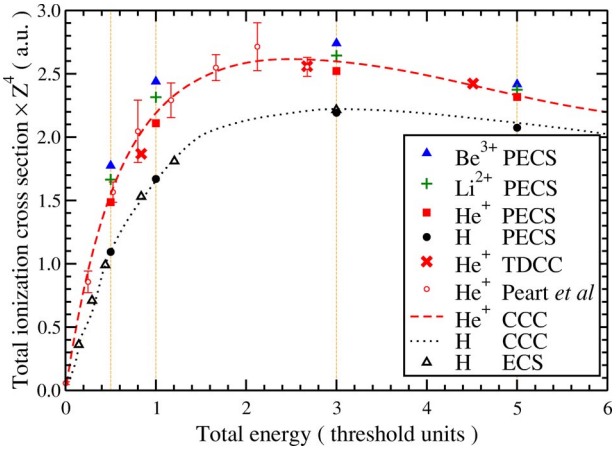


FIG. 1. TICS calculations for $Z \leqslant 4$ targets at total system energies of 0.5, 1.0, 3.0, and 5.0 t.u. The energies of our PECS calculations are indicated by vertical dashed lines. Comparison is made with ECS [8] and the $l_{\max}=4$ CCC calculations of Ref. [17] for H; CCC [11], TDCC [13], and experiment [18] for $He^+$. All TICS have been multiplied by $Z^4$.

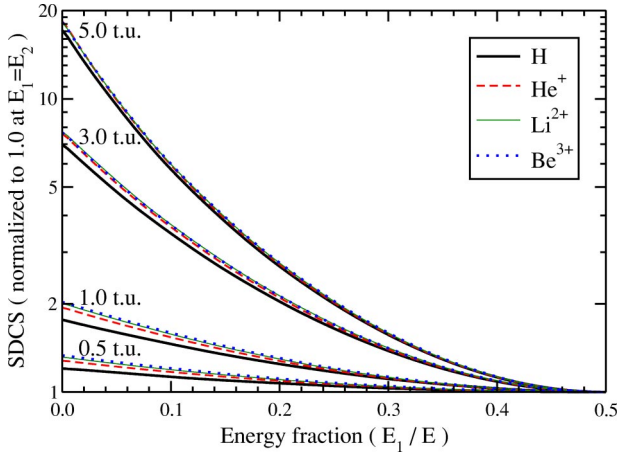


FIG. 2. SDCS calculations for $Z \leqslant 4$ targets at total system energies of 0.5, 1.0, 3.0, and 5.0 t.u. All curves have been normalized to 1.0 at equal energy sharing ($E_1=E_2$). The original SDCS can be calculated by multiplying by $\alpha(E)/Z^6$, where the normalizing constant $\alpha(E)$ is given in Table I.

$$\hat{H}_{l_i} = -\frac{1}{2}\frac{\partial^2}{\partial r_i^2} - \frac{Z}{r_i} + \frac{l_i(l_i+1)}{2r_i^2}, \tag{2}$$

and

$$\chi^{LS}_{l_1 l_2}(r_1,r_2) = \frac{i^L}{k_0}\sqrt{2\pi(2L+1)}e^{-i\sigma_L}\left\{\left(\left\langle l_1 l_2 \left\| \frac{1}{r_{12}} \right\| 0L \right\rangle_L - \frac{1}{r_2}\delta_{l_1 0}\delta_{l_2 L}\right)\phi_{1s}(Z;r_1)\psi_L(Z-1;k_0,r_2) + (-1)^S(1 \leftrightarrow 2)\right\}. \tag{3}$$

$\phi_{1s}(Z;r)$ is the radial hydrogenic ground-state wave function (multiplied by $r$) for central charge $Z$, $\psi_L(Z-1;k,r)$ is a regular Coulomb wave of charge $Z-1$ and angular momentum $L$, normalized such that $\psi_0(0;k,r)=\sin(kr)$, and $\sigma_L$ is the Coulomb wave phase shift.

These equations were solved on a finite grid with variable grid spacing. We used exterior complex scaling [16], where each radial coordinate is rotated into the complex plane at $R_0$ causing the outgoing scattering wave function to diminish exponentially. $R_0$ is made large enough to obtain convergent cross sections. The coupling of angular states $(l_1,l_2)$ was achieved using our iterative coupling method [14], and the cross sections were extracted using the surface integral method [8,14] where both asymptotic final-state continuum waves are represented by Coulomb waves of charge $Z$.

The iterative coupling method approximates the solution of Eq. (1) for each partial wave by ignoring the coupling between partial waves. The equations are then recalculated using the previous estimate of the coupled wave functions. This procedure is performed iteratively until the solutions converge, requiring of the order of 5–20 iterations for the calculations presented here. The majority of the computational effort of the PECS method is used to evaluate the propagation matrices, which are only calculated during the first iteration. Therefore, the iterative coupling of the wave functions requires little more computational effort than solving the uncoupled equations. A detailed description of this iterative coupling method is given in Ref. [14].

We present our calculations for the TICS, single-differential cross section (SDCS), and representative double-differential cross sections (DDCS), and triple-differential cross sections (TDCS) for the selected targets at the total system energies of 0.5, 1.0, 3.0, and 5.0 threshold units (t.u.). One t.u. represents the ionization threshold energy of the target and equals $Z^2/2$ atomic units (a.u.). In t.u., the impact energy is related to the total system energy by $E_0=E+1$.

Based upon our convergence studies, we estimate that our TICS calculations have a standard error of the order of 1%. To achieve this accuracy, partial waves up to $L=10$ were included in the 0.5 t.u. calculations, increasing to $L=30$ for the 5.0 t.u. calculations. The size of the grids used ranged from 100 a.u. for H at 0.5 t.u.(20.4 eV) to 15 a.u. for $Be^{3+}$ at 5.0 t.u.(1306 eV). The convergence studies undertaken for each controlled approximation in our calculations, and their contribution to the estimated standard error of our TICS calculations are: grid size $R$ (0.5%), grid spacing (0.25%), limiting partial waves $L$ (0.2%), limiting angular-momentum states $(l_1,l_2)$ for each $L$ (0.2%), and iterative coupling error

TABLE I. Normalization constants $\alpha(E)$ used in Fig. 2. To recover the original SDCS in atomic units, multiply by $\alpha(E)/Z^6$. The column energies are total system energies and are in t.u.

| | | Normalization constant $[\alpha(E)]$ | | | |
|---|---|---|---|---|---|
| $Z$ | | 0.5 t.u. | 1.0 t.u. | 3.0 t.u. | 5.0 t.u. |
| 1 | H | 8.205 | 5.611 | 1.268 | 0.4488 |
| 2 | $He^+$ | 10.93 | 6.608 | 1.397 | 0.4841 |
| 3 | $Li^{2+}$ | 12.11 | 7.141 | 1.441 | 0.4938 |
| 4 | $Be^{3+}$ | 12.84 | 7.479 | 1.502 | 0.5022 |

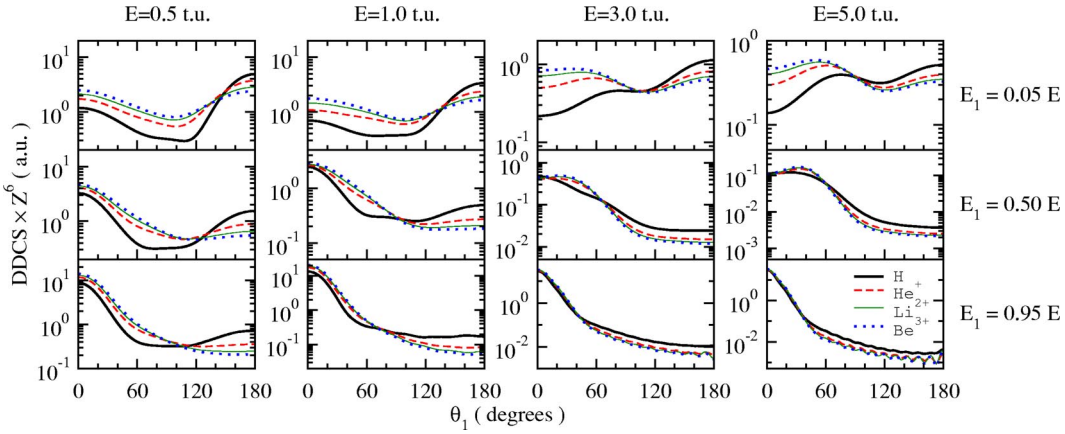


FIG. 3. DDCS calculations for $Z \leqslant 4$ targets for total system energies of 0.5, 1.0, 3.0, and 5.0 t.u.

(0.01%). It should be noted that these errors relate to the TICS, and we expect that the errors in the differential cross sections will be larger, though generally not discernible on the plots presented here. We will give a detailed analysis of our convergence studies in a later publication.

Our TICS calculations, multiplied by $Z^4$, are presented in Fig. 1. For hydrogen, our results are within 1% of the interpolated ECS and CCC calculations. Our $He^+$ calculations are within 3% of the interpolated CCC results, but systematically lower. The measurements for $He^+$ are consistent, within experimental error, with PECS, CCC, and TDCC. It should be noted that the TDCC calculations use a distorted wave perturbation calculation beyond $L=6$ and the authors claim an accuracy of the order of 5%, while the accuracy of the CCC calculations is limited by an estimation of the singlet SDCS due to oscillations inherent to the method. We should also emphasize that neither smoothing nor extrapolation procedures are used in the PECS method. The general agreement of our PECS calculations with the other theoretical calculations for hydrogen and $He^+$ gives us confidence that our estimated error is justified.

It is clear from our calculations that by $E=5.0$ t.u. the scaled TICS are converging quickly with increasing $Z$, and that the rate of convergence decreases with decreasing energy. This gives support to the $Z^4$ scaling law [2] for TICS, for large $Z$ or high $E$.

Normalized SDCS at the selected energies are shown in Fig. 2. They reveal a systematic increase in the contribution to the SDCS at asymmetric energy sharing with increasing scaled system energy. Like the TICS, the shape of the SDCS converges quickly with increasing $Z$ at high energies, but more slowly with decreasing scaled system energy. In Table I we have included the normalization constants used to scale the plots in Fig. 2, from which our unscaled SDCS results can be derived. These constants have been divided by $Z^6$, and show similar convergence behavior to the TICS. This supports the $Z^6$ scaling law for differential cross sections of hydrogenic targets, for large $Z$ or high $E$.

Our DDCS results are plotted in Fig. 3 for selected secondary electron energies and total system energies. The shape of the DDCS begins to converge with increasing $Z$, and this convergence is more rapid with increasing scaled

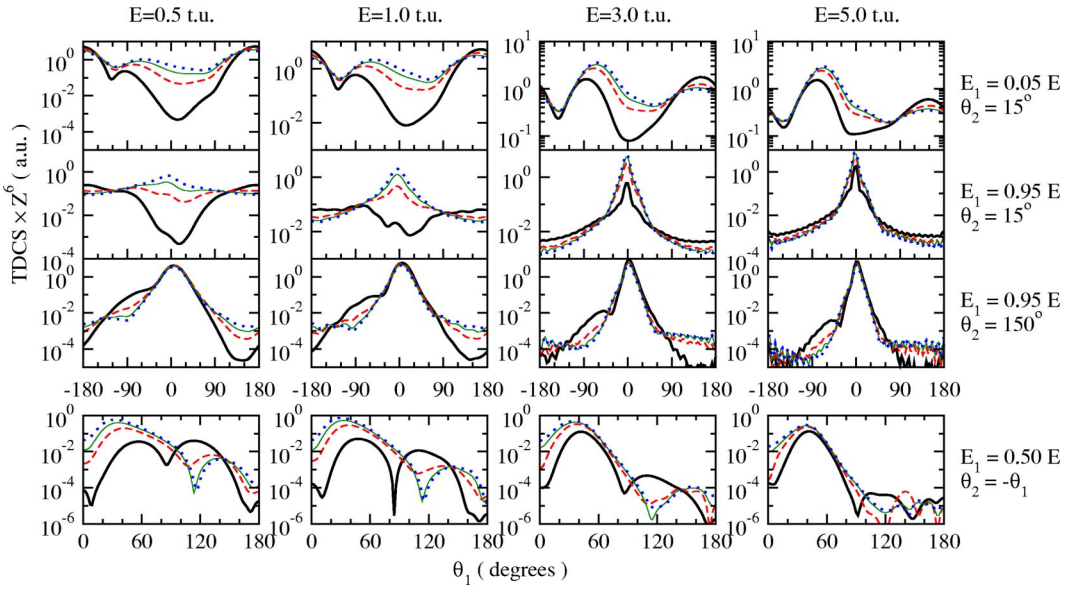


FIG. 4. Coplanar TDCS calculations for $Z \leqslant 4$ targets for total system energies of 0.5, 1.0, 3.0, and 5.0 t.u.The curves are as labeled in Fig. 3.

system energy. Electrons ejected at low energy are more spatially dispersed than high-energy electrons, and the dominance of back scattering of low-energy electrons decreases with increasing $Z$ and increasing system energy. The high-energy electrons are ejected in a narrow peak near zero degrees, which narrows with increasing energy.

In Fig. 4 our coplanar TDCS results are plotted for selected scaled total system energies and selected secondary electron energies and directions. The shape of the TDCS plots also converges with increasing $Z$, consistent with a $Z^6$ scaling law for differential cross sections, and converge more rapidly with increasing scaled system energy. At $E \leqslant 1.0$ t.u., there is a marked difference in the spatial distribution of the fast outgoing electron, when the slow electron is forward scattered at 15°; for atomic hydrogen the minima in the TDCS is in the forward direction, whereas the charged targets have a maxima in this direction. The slight oscillations in the TDCS of the back-scattered fast electron for $E \geqslant 3$ t.u., which are suppressed by 2–5 orders of magnitude relative to the peak, are expected to diminish as partial waves $L > 30$ are included. These very high partial waves were not included in these calculations as they have not converged sufficiently at the grid size selected.

In conclusion, we have used our PECS method, with iterative coupling, to calculate highly accurate total and differential ionization cross sections for charged hydrogenic targets with low $Z$ at low to moderate energies. The PECS method with iterative coupling proved to be highly efficient, providing an estimated 100-fold reduction in total computation time compared with the PECS method using direct coupling. Our computations support a $Z^4$ scaling law for TICS and $Z^6$ scaling of differential cross sections, for large $Z$ or high $E$, over a wide range of kinematics. Our results are also consistent with the analysis of available experimental results for hydrogenic targets by Tinschert *et al.* [19] (as discussed in Ref. [2]), who suggested that the scaling laws become valid for $E_0 > (Z/2)^2 \times 500$ eV.

We would like to thank Igor Bray for supplying tabulated CCC results, and acknowledge the support of the Australian Research Council, the Australian Partnership for Advanced Computing, and the Western Australian Interactive Virtual Environments Centre.

[1] A. Burgess, D. G. Hummer, and J. A. Tully, Philos. Trans. R. Soc. London, Ser. A **266**, 225 (1970).
[2] C. R. Stia, O. A. Fojón, and R. D. Rivarola, J. Phys. B **33**, 1211 (2000).
[3] J. J. Thomson, Philos. Mag. **23**, 449 (1912).
[4] S. M. Younger, Phys. Rev. A **22**, 111 (1980).
[5] D. Fang, W. Hu, J. Tang, Y. Wang, and F. Yang, Phys. Rev. A **47**, 1861 (1993).
[6] X. Jia, Q. Shi, Z. Chen, J. Chen, and K. Xu, Phys. Rev. A **55**, 1971 (1997).
[7] M. Brauner, J. S. Briggs, and H. Klar, J. Phys. B **22**, 2265 (1989).
[8] M. Baertschy, T. N. Rescigno, and C. W. McCurdy, Phys. Rev. A **64**, 022709 (2001).
[9] I. Bray, J. Phys. B **36**, 2203 (2003).
[10] J. Colgan, M. S. Pindzola, F. J. Robicheaux, D. C. Griffin, and M. Baertschy, Phys. Rev. A **65**, 042721 (2002).
[11] I. Bray, I. E. McCarthy, J. Wigley, and A. T. Stelbovics, J. Phys. B **26**, L831 (1993).
[12] J. Colgan, M. S. Pindzola, and F. Robicheaux, Phys. Rev. A **66**, 012718 (2002).
[13] M. C. Witthoeft, M. S. Pindzola, and J. Colgan, Phys. Rev. A **67**, 032713 (2003).
[14] P. L. Bartlett, A. T. Stelbovics, and I. Bray, J. Phys. B **37**, L69 (2004).
[15] P. L. Bartlett and A. T. Stelbovics, Phys. Rev. A **69**, 022703 (2004).
[16] T. N. Rescigno, M. Baertschy, D. Byrum, and C. W. McCurdy, Phys. Rev. A **55**, 4253 (1997).
[17] K. Bartschat and I. Bray, J. Phys. B **29**, L577 (1996).
[18] B. Peart, D. S. Walton, and K. T. Dolder, J. Phys. B **2**, 1347 (1969).
[19] K. Tinschert, A. Muller, G. Hofmann, K. Huber, R. Becker, D. C. Gregory, and E. Salzborn, J. Phys. B **22**, 531 (1989).